# Two Pif1 Family DNA Helicases Cooperate in Centromere Replication and Segregation in *Saccharomyces cerevisiae*

**Chi-Fu Chen,* Thomas J. Pohl,* Sebastian Pott,† and Virginia A. Zakian*,[1]**
*Department of Molecular Biology, Lewis Thomas Laboratory, Princeton University, New Jersey 08544 and †Department of Human Genetics, University of Chicago, Illinois 60637

**ABSTRACT** Pif1 family helicases are found in virtually all eukaryotes. *Saccharomyces cerevisiae* (Sc) encodes two Pif1 family helicases, ScPif1 and Rrm3. ScPif1 is multifunctional, required not only for maintenance of mitochondrial DNA but also for multiple distinct nuclear functions. Rrm3 moves with the replication fork and promotes movement of the fork through ~1400 hard-to-replicate sites, including centromeres. Here we show that ScPif1, like Rrm3, bound robustly to yeast centromeres but only if the centromere was active. While Rrm3 binding to centromeres occurred in early to mid S phase, about the same time as centromere replication, ScPif1 binding occurred later in the cell cycle when replication of most centromeres is complete. However, the timing of Rrm3 and ScPif1 centromere binding was altered by the absence of the other helicase, such that Rrm3 centromere binding occurred later in *pif1-m2* cells and ScPif1 centromere binding occurred earlier in *rrm3*Δ cells. As shown previously, the modest pausing of replication forks at centromeres seen in wild-type cells was increased in the absence of Rrm3. While a lack of ScPif1 did not result in increased fork pausing at centromeres, pausing was even higher in *rrm3*Δ *pif1*Δ cells than in *rrm3*Δ cells. Likewise, centromere function as monitored by the loss rate of a centromere plasmid was increased in *rrm3*Δ but not *pif1*Δ cells, and was even higher in *rrm3*Δ *pif1*Δ cells than in *rrm3*Δ cells. Thus, ScPif1 promotes centromere replication and segregation, but only in the absence of Rrm3. These data also hint at a potential post-S phase function for ScPif1 at centromeres. These studies add to the growing list of ScPif1 functions that promote chromosome stability.

**KEYWORDS** Pif1; Rrm3; helicase; centromere; Pfh1

MEMBERS of the Pif1 family of 5′-to-3′ ATP-dependent DNA helicases are present in almost all eukaryotes and many bacteria (Bochman *et al.* 2011; Chung 2014; Geronimo and Zakian 2016). They are distinguished by a 23-amino acid segment called the Pif1 signature motif, which is unique to Pif1 family helicases and essential for the ATPase activity of both the *Saccharomyces cerevisiae* (Sc) Pif1 and *Schizosaccharomyces pombe* Pfh1, its fission yeast homolog (Geronimo *et al.* 2018; Mohammad *et al.* 2018).


doi: https://doi.org/10.1534/genetics.118.301710
Manuscript received August 17, 2018; accepted for publication November 6, 2018; published Early Online November 15, 2018.
Available freely online through the author-supported open access option.
Supplemental material is available online at Figshare: https://doi.org/10.25386/genetics.7335188.
[1]Corresponding author: Department of Molecular Biology, Washington Rd., Lewis Thomas Laboratory, Princeton University, Princeton, NJ 08544. E-mail: vzakian@princeton.edu

Unlike most eukaryotes, including *S. pombe* and humans, *S. cerevisiae* encodes two Pif1 family helicases, ScPif1 and Rrm3. ScPif1 is multifunctional (Bochman *et al.* 2011; Chung 2014; Geronimo and Zakian 2016); it maintains mitochondrial DNA, inhibits telomerase at telomeres and double-strand breaks, processes Okazaki fragments, blocks fork progression at the replication fork barrier (RFB) in ribosomal DNA (rDNA), and promotes break-induced replication repair of double-strand breaks. Rrm3 promotes replication fork progression at ~1400 discrete sites, most or all of which are bound by stable DNA–protein complexes (Ivessa *et al.* 2003; Torres *et al.* 2004). Rrm3-sensitive sites include the RFB in rDNA, RNA polymerase III-transcribed genes, inactive replication origins, silent mating type loci, telomeres, converged replication forks, and centromeres (Ivessa *et al.* 2000, 2002, 2003; Azvolinsky *et al.* 2009). Rrm3 is part of the replisome, and hence moves with the replication fork through Rrm3-sensitive and Rrm3-insensitive sites

(Azvolinsky *et al.* 2009), as does fission yeast Pfh1 (McDonald *et al.* 2016). In contrast, ScPif1 is recruited to its sites of action after their replication (Paeschke *et al.* 2011) (this paper). Although Rrm3 is best known for its role in fork progression, it also restricts DNA replication during replication stress by binding to Orc5 (Syed *et al.* 2016) and functions in the repair of replication-generated double-strand breaks (Muñoz-Galván *et al.* 2017).

Although ScPif1 and Rrm3 affect many of the same genomic loci, they were initially thought to have largely nonoverlapping functions at their common sites of action (Bessler *et al.* 2001). For example, while ScPif1 inhibits telomerase-mediated telomere lengthening, Rrm3 promotes semiconservative replication of telomeric DNA (Zhou *et al.* 2000; Ivessa *et al.* 2002). More recently, ScPif1 and Rrm3 were shown to have overlapping functions at certain loci, with one of the two affecting the site only when the other helicase is absent. For example, ScPif1 promotes replication and suppresses DNA damage at G-quadruplex (G4) motifs, while Rrm3 does so only in cells lacking ScPif1 (Paeschke *et al.* 2013). Likewise, Rrm3 promotes replication past tRNA genes (tDNAs), as does ScPif1 in *rrm3*Δ cells (Osmundson *et al.* 2017; Tran *et al.* 2017).

Of the Pif1 family DNA helicases, ScPif1 is the most extensively characterized *in vitro*. Although ScPif1 has low activity on 5′-tailed duplex DNA molecules, it efficiently unwinds forked molecules, G4 structures, and RNA–DNA hybrids (Boulé *et al.* 2005; Boulé and Zakian 2007; Ribeyre *et al.* 2009; Paeschke *et al.* 2013; Zhou *et al.* 2014). ScPif1 can also displace stably bound protein from DNA (Koc *et al.* 2016) and promotes the processivity of DNA polymerase δ (Wilson *et al.* 2013; Buzovetsky *et al.* 2017). Pfh1 also efficiently unwinds G4 structures and RNA–DNA hybrids, and can displace proteins from DNA (Wallgren *et al.* 2016; Mohammad *et al.* 2018). In contrast, very little biochemistry has been done on Rrm3 owing to difficulties purifying the protein.

In this study, we show that, like Rrm3, ScPif1 functions at yeast centromeres. Centromeres are the platform for kinetochore assembly and subsequent microtubule attachment, and thus are essential for chromosome segregation in mitosis and meiosis. Centromeres also support sister chromatid cohesion at pericentric DNA, which keeps sister chromatids together until anaphase. In budding yeast, centromeres facilitate the activation of flanking origins of replication in early S phase (Pohl *et al.* 2012; Natsume *et al.* 2013).

The *S. cerevisiae* centromere is remarkably small, consisting of only ~125 bp. Although the 16 yeast centromeres vary somewhat in primary sequence, each contains three conserved elements: CDEI (8 bp; important but not essential for centromere function), CDEII (78–86 bp and highly A–T-rich; essential for centromere function) and CDEIII (25 bp; essential for centromere function) [see Biggins (2013) for a review of budding yeast centromeres and their associated proteins] (Figure 1A). CDEI is bound by Cbf1, which is also a transcription factor for certain RNA polymerase II-transcribed genes (Mellor *et al.* 1990). CDEII binds a nucleosome containing Cse4, the centromere-dedicated histone H3 (CENP-A in humans). CDEIII is bound by Cbf3, a complex of four essential proteins that is required for the association of kinetochore proteins with centromere DNA (Biggins 2013). The multiprotein kinetochore complex is assembled on centromeric DNA throughout most of the cell cycle, including during S phase (Greenfeder and Newlon 1992).

Budding yeast centromeres replicate relatively early in S phase (McCarroll and Fangman 1988). In wild-type (WT) cells, replication forks pause transiently at centromeres (Greenfeder and Newlon 1992), and this pausing increases two- to threefold in *rrm3*Δ cells (Ivessa *et al.* 2003). By analogy to other Rrm3-affected sites, Rrm3 probably assists the fork in moving past the multiprotein kinetochore complex (Ivessa *et al.* 2003). Tof1 is a checkpoint-mediator protein that associates with the replisome. Its presence is important for pausing at multiple natural pause sites, including centromeres, where it is thought to stabilize the protein complexes that impede fork progression (Mohanty *et al.* 2006; Hodgson *et al.* 2007).

Here, we show that not only Rrm3 but also ScPif1 bind centromeres *in vivo*, and that the binding of both helicases to centromeres is cell cycle regulated. In WT cells, Rrm3 binding was highest from early to mid-S phase, while ScPif1 binding peaked in late S/G2 phase, suggesting that the helicases have different centromere functions. However, ScPif1 promotes the replication of centromeric DNA and the segregation of centromere plasmids in *rrm3*Δ (but not WT) cells, indicating that it can partially compensate for loss of Rrm3 for these functions.

## Materials and Methods

### *Yeast strains*

Yeast strains were derivatives of YPH499 (See Supplemental Material, Table S1). Yeast strains, plasmids, and primers are listed in Table S1 and S2. Experiments were carried out in YPH499 unless otherwise indicated. Epitope tagging to generate ScPif1-Myc13, Rrm3-Myc13, ScPif1-K264A-Myc13, and Rrm3-K260A-Myc13 was carried out as described (Ivessa *et al.* 2002; Paeschke *et al.* 2011). Each deletion eliminated the entire ORF. The *pif1-m2* allele, which was made as described in Schulz and Zakian (1994), has WT mitochondrial function but is deficient, although not null, for nuclear functions.

### *Chromatin immunoprecipitation-sequencing alignment, peak calling, and preparation of browser snapshots*

ScPif1 and Rrm3 chromatin immunoprecipitation (ChIP) samples and input DNA samples were converted to an Illumina sequencing library (Illumina, San Diego, CA) using the automated Apollo 324TM NGS Library Prep System and the PrepX DNA library kit (Wafergen, Fremont, CA) according to the manufacturer's instructions, which included DNA end repair, A-tailing, adapter ligation, and limited amplification. To

facilitate multiplexing, adaptors contained a library-specific barcode. The libraries were examined on Bioanalyzer (Agilent, CA) DNA high sensitivity (HS) chips for size distribution, and quantified by Qubit fluorometer (Invitrogen, Carlsbad, CA). Libraries were pooled together at equal molar amounts and sequenced on an Illumina HiSeq 2500 Rapid Flowcell as single-end 65-nt reads, along with 7-nt Index reads, following the manufacturer's protocol. Raw sequencing reads were filtered by Illumina HiSeq Control Software to generate pass-filter reads for further analysis.

Reads were aligned to the *S. cerevisiae* genome (assembly SacCer3) using bowtie2 (version 2.2.6.2) (Langmead and Salzberg 2012). For subsequent analyses, reads were extended to 300 bp to reflect the empirical fragment length and all libraries were downsampled to contain 10 M reads. Average ChIP-seq (ChIP-sequencing) signals around centromere regions were determined using the function ScoreMatrixBin in the R package genomation (Akalin *et al.* 2015). Sequencing reads averaged across 2-kb windows centered on the middle of the centromeric intervals that were split into 5-bp bins. ChIP-seq data were visualized as custom tracks on the University of California Santa Cruz genome browser (Kent *et al.* 2002). For display, sequencing reads were converted into bedgraph files capturing genome-wide per-base coverage using the genomecov function from the BEDTools suite (Quinlan and Hall 2010).

### *ChIP and quantitative PCR*

Epitope tagging of proteins for ChIP experiments was carried out as previously described (Tran *et al.* 2017). Briefly, cells were grown in 50 ml of YEPD (YEP with dextrose) overnight and harvested at an $OD_{660}$ of 0.5. Cells were cross-linked with 1% formaldehyde for 10 min. Chromatin purification was carried out as described (Paeschke *et al.* 2011), except that DNA was sheared to an average size of 300 bp using an E220 evolution Focused-ultrasonicator (Covaris, Woburn, MA). Anti-MYC monoclonal antibody (#631206; Clontech) was diluted to 0.02 μg/μl and coupled to 80 μl of Dynabeads protein G (#10004D; Thermo Fisher Scientific). Reverse-cross-linking DNA was performed and purified by QIAquick PCR Purification kit (#28106; QIAGEN, Valencia, CA). Immunoprecipitated chromatin and input DNA were analyzed by quantitative PCR (qPCR) using iQ SYBR Green Supermix (#170–8882; Bio-Rad, Hercules, CA) and a CFX96 real-time system (Bio-Rad). All ChIP experiments were repeated at least three times. Strains and primers are listed in Table S1 and S2. WT cells without a Myc-tagged protein were used as a negative control. Most ChIP-qPCR were quantified by $[(\text{ChIP/Input})_{\text{Target site}}/(\text{ChIP/Input})_{YBL028C}]$. *YBL028C* is a control sequence that has very low ScPif1 and Rrm3 binding.

### *Cell synchrony*

For ChIP and RT-PCR experiments, the synchronization method and FACS analysis were as previously described (Azvolinsky *et al.* 2006). Briefly, single colonies were grown in YEPD overnight at 30°. Cells were diluted and grown overnight to an $OD_{660}$ of 0.15. α-Factor (Princeton University) was added to cultures (0.015 ng/ml) and cells were incubated for 3–4 hr at 24° until microscopic examination indicated that ~90% of cells were unbudded. Cells were collected and washed in YEPD. Cells were resuspended in fresh YEPD containing 70 μg/ml Pronase (Sigma [Sigma Chemical], St. Louis, MO) at 24° and collected at the indicated time points. The quality of each synchrony was monitored by flow cytometry. Each synchrony was done at least three times on independent colonies.

### *Flow cytometry*

Cells were fixed with 70% EtOH and stored at 4° overnight. Cells were then pelleted, washed, and suspended in 50 mM sodium citrate and sonicated. RNase A was added at a final concentration of 0.25 mg and cells were incubated for 1 hr at 50°. One milligram of Proteinase K (Roche) was added and cells were incubated for an additional 1 hr at 50°. Nuclear DNA was stained with Sytox Green (2 μM) (Invitrogen) at room temperature. Samples were analyzed in an LSRII (BD Biosciences, Jose, CA) using FACSDiVa software for data acquisition. Sytox green dye was excited with a 488-nm laser and the emitted fluorescence was collected through a 525/50 bandpass filter. FlowJo V.10 (FlowJo LLC, Ashland, OR) software was used for cell cycle analysis. Statistical significance was determined by two-tailed Student's *t*-test.

### *Plasmid loss-rate assay*

Plasmid loss assays measure the cumulative loss of a pRS316 from a yeast culture over ~around eight generations of growth in nonselective media. An overnight culture of cells was grown with pRS316 in URA media. The cells were inoculated into 3 ml YEPD medium and grown to saturation (around eight generations of growth). The cells were diluted with water, and plated on YEPD and plates with complete medium lacking uracil (~250 cells/plate). Cells were grown for 3 days (or as needed) and colonies counted. Each experiment was done at least three times. The plasmid loss rate (% loss per generation) was determined by $1-(F/I)^{1/N}$, where I is the initial percentage of plasmid-containing cells and F is the percentage of plasmid-containing cells after N generations (Gibson *et al.* 1990).

### *Two-dimensional agarose gel electrophoresis*

Replication intermediates were analyzed by standard two-dimensional (2D) agarose gel electrophoresis techniques performed on total genomic DNA isolated from asynchronous cells (Brewer and Fangman 1987, 1991; Huberman *et al.* 1987). Cells were collected in log phase at an optical density of OD660 of ~0.6. Collected DNA was restriction enzyme digested (see Figure 4 legend for specific enzyme). In the first dimension, DNA was separated in 0.4% agarose at room temperature for 20 hr at 2.0 V/cm. The second dimension was run for 15 hr in 1.1% agarose containing ethidium bromide (0.3 μg/ml) at 4.4 V/cm at 4°. Southern blots were probed

using a $^{32}$P-labeled probe, whose position is indicated in Figure 4. The extent of pausing was obtained in the following manner. The $^{32}$P signal corresponding to the pause was obtained using ImageQuant TL software to determine the $^{32}$P intensity of the pause. The background signal was obtained by measuring $^{32}$P intensity from an equal area of the blot at a location that was offset from the pause site so as not to contain signal from the *y*-arc. This value was then subtracted from the overall $^{32}$P intensity of the pause to remove background. The same steps were taken for a portion of the ascending *y*-arc. The intensity of the pause for a given blot was obtained by subtracting *y*-arc signal (minus background) from the pause signal (minus background). Quantification of pausing was done in two different biological replicates and was normalized to the WT pause signal to obtain the fold increase in the pause in a mutant strain relative to pausing in the otherwise isogenic WT strain.

### Benomyl and nocodazole sensitivity

Sensitivity to nocodazole (10 μg/ml) or benomyl (10 μg/ml) was tested by growing cells overnight in YEPD at 30°. Strains were then spotted in fivefold serial dilutions from $3\times10^7$ cells per spot on YEPD plates with and without nocodazole or benomyl.

The experiments for ChIP-qPCR of benomyl-treated cells are described briefly below. Cells were grown to an $OD_{660}$ of 0.3. Cells were diluted and treated with DMSO (control, 0.1%) or benomyl (10 μg/ml) in YEPD liquid media and grown overnight. The cells were collected at an $OD_{660}$ of ~1. The ChIP-qPCR was the same as in other experiments.

### Data availability

Strains and plasmids are available upon request. The authors affirm that all data necessary for confirming the conclusions of the article are present within the article, figures, and tables. Supplemental material available at Figshare: https://doi.org/10.25386/genetics.7335188.

## Results

### ScPif1 and Rrm3 helicases bind robustly to yeast centromeres

Although Rrm3 binds to all nuclear sequences at their time of replication, its binding is elevated at hard-to-replicate sites, including centromeres (Azvolinsky *et al.* 2006, 2009). Because these sites also contain elevated levels of DNA polymerase II (DNA Pol2), the leading-strand DNA polymerase, we interpret the higher levels of Rrm3 as due to pausing at hard-to-replicate sites, as high DNA Pol2 occupancy correlates with pause sites seen by 2D gels. Earlier genome-wide studies using ChIP and microarrays (ChIP-chip) did not detect ScPif1 binding to centromeres (Paeschke *et al.* 2011). However, using ChIP in combination with DNA sequencing (ChIP-seq), we found robust ScPif1 binding to all 16 yeast centromeres in asynchronous cells (C.-F. Chen, S. Pott and V. A. Zakian, personal communication). In all instances, this binding was centered on the 125-bp centromere and, typically, it was the strongest ScPif1-binding site within 5 kb to either side of the centromere (Figure 1, B and C). Elevated binding of Rrm3 to centromeres was also seen in genome-wide ChIP-seq studies using myc-Rrm3 (Figure 1, B and C).

To confirm ScPif1 and Rrm3 binding to centromeres, we performed ChIP followed by real-time qPCR (ChIP-qPCR) on 6 of the 16 native yeast centromeres, CENs 3, 6, 11, 12, and 14 (Figure 1D), and to an ectopic copy of CEN7 (Figure 2B). For these studies, cells were grown at 30°. The binding of ScPif1 and Rrm3 was normalized to a control sequence, *YBL028C*, which binds little or no ScPif1 or Rrm3 (Tran *et al.* 2017). Although the level of binding varied somewhat from centromere to centromere, ScPif1 and Rrm3 each bound strongly to all six centromeres.

Using asynchronous cells growing at 30°, we also examined the binding of each helicase in the absence of the other. The level of ScPif1 binding to centromeres 3, 6, 11, 12, and 14 was the same in WT and *rrm3*Δ cells ($P > 0.05$) (Figure 1D). Likewise, the level of Rrm3 binding to these centromeres was not affected significantly by the absence of ScPif1 ($P > 0.05$) (Figure 1D).

Because Tof1 stabilizes replication forks at centromeres and antagonizes the helicase activity of Rrm3 at the RFB (Mohanty *et al.* 2006; Hodgson *et al.* 2007), we asked if the levels of ScPif1 or Rrm3 centromere binding were altered in 30°-grown *tof1*Δ cells (Figure 1E). Rrm3 was significantly higher at CEN3, 6, 12, and 13 in *tof1*Δ compared to WT cells ($P \leq 0.01$). However, ScPif1 centromere binding was not affected significantly by the absence of Tof1 ($P > 0.05$) (Figure 1E). These results suggest that Tof1 and Rrm3 centromere binding is competitive, consistent with the two proteins acting antagonistically at centromeres as they do at the RFB (Mohanty *et al.* 2006). The data also hint that ScPif1 and Rrm3 may have different centromere functions, as in otherwise WT cells, levels of ScPif1 binding to centromeres was not affected by the absence of *TOF1* (Figure 1E).

### ScPif1 and Rrm3 bind poorly to an inactive centromere

As a first step in determining the role of ScPif1 binding to centromeres, we asked if its binding required a functional centromere. For this experiment, we grew cells at 30° and used strains with a modified version of chromosome XIV that contain an active or an inactive CEN7 (Pohl *et al.* 2012) (Figure 2A). Both the active and inactive CEN7 are inserted within the *MET2* locus. In the strain harboring the active CEN7, the native CEN14 was replaced with *URA3*. The inactive CEN7 has a 3-nt substitution in the essential CDEIII motif that eliminates CEN function (Pohl *et al.* 2012). Again, we used epitope-tagged ScPif1 (or Rrm3) and ChIP-qPCR in asynchronous cells to determine if helicase binding was dependent on CEN activity. ScPif1 and Rrm3 bound strongly to the functional CEN7, but the binding of both helicases was significantly lower at inactive CEN7 (Figure 2B, $P < 0.001$).

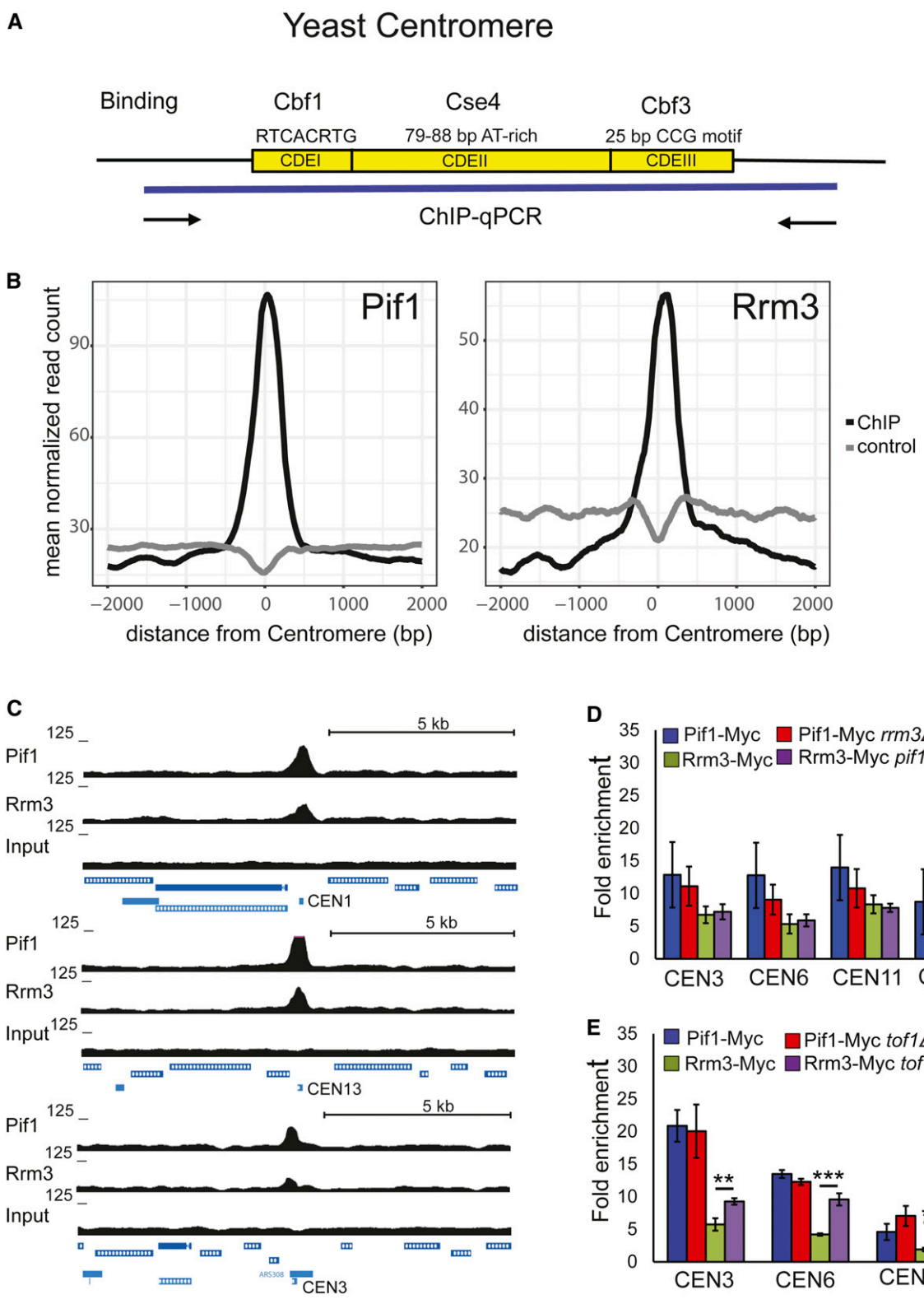


**Figure 1** ScPif1 and Rrm3 helicases bind robustly to yeast centromeres. (A) Schematic of the three conserved elements in the ~125-bp budding yeast centromere: (1) CDEI is 8-bp long; its consensus is RTCACRTG (R = purine); (2) CDEII is 78–86-bp long and is A+T-rich; and (3) CDEIII is 25-bp long; its consensus is (TGTTT(T/A)TGNTTTCCGAAANNNAAAAA), where N is any nucleotide (Biggins 2013). (B) Average normalized ScPif1 and Rrm3 ChIP-seq read counts are plotted at centromeric regions. Reads from matched input samples that were sheared but did not undergo the ChIP procedure were used as a control. (C) ChIP-seq signal for ScPif1 and Rrm3 (upper panel). Lower panels show ScPif1 and Rrm3 ChIP-seq read density at three centromeres (CEN1, CEN13, and CEN3). UCSC browser tracks were used to visualize ScPif1 binding and control reads (input). Data represent combined reads of three independent replicates. All data were normalized to 10 M reads per library. (D) Using Myc-tagged ScPif1 and Rrm3, ChIP-qPCR was carried out on

### *Robust binding of ScPif1 to CEN7 does not require its catalytic activity*

To ask if catalytically inactive ScPif1 or Rrm3 bound centromeres (Figure 2C), we used two helicase-inactive alleles, *ScPIF1*-K264A and *RRM3*-K260A, in which the invariant lysines in the Walker A box are mutated (Ivessa *et al.* 2000; Zhou *et al.* 2000). Both alleles produce stable but catalytically inactive protein. ScPif1-K264A bound active CEN7 as well as WT ScPif1 (Figure 2C), consistent with results from ChIP-seq where WT and ScPif1-K264A bind equally well to all of its *in vivo* targets (Chen *et al.*, personal communication). In contrast, binding of WT Rrm3 was ∼5.3 times higher than Rrm3-K260A to CEN7 (Figure 2, C and D).

To determine if the reduced binding of Rrm3-K260A was specific for centromeres, we compared the binding of mutant and WT Rrm3 to several well-characterized Rrm3 substrates, three tDNAs, and the right telomere of chromosome VI (Ivessa *et al.* 2003) (Figure 2D). The three tDNAs are particularly Rrm3-sensitive, owing to replication and transcription moving through the genes in opposite directions ("head-on" orientation) (Ivessa *et al.* 2003; Tran *et al.* 2017). Similar to what was seen at CEN7, the level of WT Rrm3 binding was significantly higher at the three tDNAs and at the VI-R telomere than binding of Rrm3-K260A ($P < 0.01$). However, the fold difference in binding ranged from ∼1.7- (tDNA$^{gly}$ Tel VI-R) to around eightfold (tRNA$^{tyr}$)-higher binding of WT Rrm3 compared to the Rrm3-K260A-binding level. Thus, the inactive Rrm3-K260A binds Rrm3-sensitive sites but not to the same extent as WT Rrm3.

### *ScPif1 and Rrm3 binding to centromeres is cell cycle regulated*

Because ScPif1 and Rrm3 binding was dependent on the presence of an active centromere (Figure 2), we considered the possibility that they might bind centromeres in a cell cycle-dependent manner, and that their time of binding might provide clues about their centromere functions. For example, if the helicases promote centromere replication, they would likely bind in early–mid-S phase, as this is the time when most yeast centromeres replicate (McCarroll and Fangman 1988). Alternatively, or in addition, the two helicases might bind centromeres in mitosis, when they carry out their segregation functions, such as attaching to the mitotic spindle or loss of sister centromere cohesion. To examine ScPif1 and Rrm3 binding throughout the cell cycle, we arrested cells in late G1 phase by incubating them in the presence of α-factor. Cells were then released from α-factor arrest to allow them to move through S phase in a synchronous manner. Cells were collected at 15-min intervals throughout the succeeding S/G2/M phases, and occupancy of ScPif1 and Rrm3 was determined by ChIP-qPCR at each time point (Figure 3 and Figure S1). As is typical for synchrony experiments, cells were grown at 24° to provide better resolution of cell cycle-regulated events. As a result, the ChIP-seq values for these experiments were lower than in asynchronous cells, which were grown at 30° (Figure 1). Likewise, when ChIPs for Rrm3- or Pif1-centromere binding were conducted at 24° in asynchronous cells, ChIP values were lower than for the same experiment at 30° (Figure S2).

Rrm3 moves with the replication fork so its time of binding provides a marker for the time of centromere replication (Azvolinsky *et al.* 2006). Although the average time of centromere replication as determined by density transfer experiments occurs relatively early in S phase (McCarroll and Fangman 1988), the time of replication of any given centromere in a population of cells occurs over a fairly broad portion of S phase. For example, CEN3 overlaps with the early activating origin *ARS308*, making it one of the earliest replicating sequences in the yeast genome (McCarroll and Fangman 1988; Pohl *et al.* 2012). In fact, ∼15% of CEN3 molecules replicate in late G1 phase (McCarroll and Fangman 1988). However, even for CEN3, individual CEN3 molecules replicate over a 15-min interval of the 30–40-min S phase (McCarroll and Fangman 1988).

Consistent with its very early replication, Rrm3 binding to CEN3 was highest at 15 min (the very beginning of S phase) and 30 min (early S phase) (red circles; Figure 3A). CEN12, located immediately adjacent to early activating origin *ARS1208*, replicates later than CEN3 but still replicates in early S phase (McCarroll and Fangman 1988; Pohl *et al.* 2012). Peak Rrm3 binding to CEN12 was also observed at early S phase (30 min; red circles; Figure 3E). Rrm3 binding to CEN11 was uniformly high from 0 to 45 min, suggesting that replication of CEN11 occurred throughout S phase (Figure 3C, red circles). In previous studies, CEN11 has replicated considerably later than CEN3, and individual CEN11 molecules have replicated over about one-half of the S phase (McCarroll and Fangman 1988).

Although the timing of centromere replication as deduced from the time of Rrm3 binding differed from centromere to centromere, the cell cycle pattern of peak ScPif1 binding was largely nonoverlapping with peak binding of Rrm3 at all three centromeres. Thus, at CEN3, ScPif1 binding occurred mainly in late S/G2 phase (60–75 min; Figure 3B, blue squares) compared to 15–30 min for Rrm3 binding (Figure 3A, red circles). The peak of ScPif1 binding to CEN12 also occurred in late S/G2 phase (60 min; Figure 3F, blue squares), while the peak of ScPif1 binding to CEN11 was even

three independent isolates of WT, *pif1*Δ, and *rrm3*Δ asynchronous cells grown at 30°. Binding to CEN3, 6, 11, 12, and 14 was normalized to binding to *YBL028C*, a control sequence that has low binding to both helicases (Tran *et al.* 2017). Fold enrichment is [(ChIP/Input)$_{\text{Target site}}$/(ChIP/Input)$_{YBL028C}$]. Blue bars, ScPif1 binding in WT cells; red bars, ScPif1 binding in *rrm3*Δ cells; green bars, Rrm3 binding in WT cells; purple bars, Rrm3 binding in *pif1*Δ cells. Here and elsewhere, error bars are ± SD, and *P*-values were obtained using an unpaired two-tailed Student's *t*-test. In all figures, * $P \leq 0.05$, ** $P \leq 0.01$, *** $P \leq 0.001$, and **** $P \leq 0.0001$. (E) ChIP-qPCR was performed as described in (D), except that binding was determined in WT and *tof1*Δ cells. ChIP, chromatin immunoprecipitation; ChIP-seq, ChIP-sequencing; qPCR, quantitative PCR; UCSC, University of California Santa Cruz; WT, wild-type.

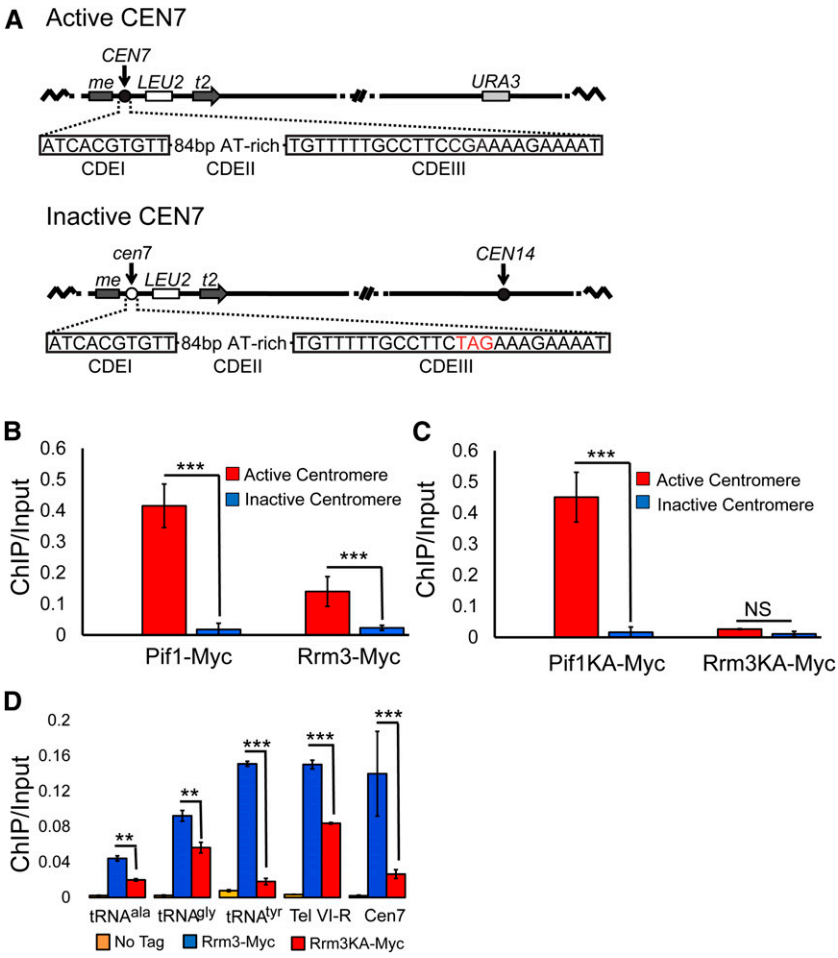


**Figure 2** ScPif1 and Rrm3 bind poorly to an inactive CEN7. (A) Diagram of the structure of active (CEN7) and inactive (cen7) centromeres, and their positions on chromosome XIV. The nucleotides in red are the changes that eliminate CEN7 function. (B) ChIP-qPCR was used to determine the levels of ScPif1 and Rrm3 binding to active CEN7 (red bars) and inactive cen7 (blue bars). (C) Helicase-inactive ScPif1 but not helicase-inactive Rrm3 binds active CEN7. The experiment is the same as in (B), except that binding of helicase-inactive proteins, ScPif1-K264A and Rrm3-K260A, was monitored. Untagged strains, which were used as negative controls, are not shown because there was no visible binding at this scale. (D) Binding of Rrm3-Myc and Rrm3-K260A-Myc to other Rrm3-sensitive sites; three tRNA sites [*tDNA$^{ala}$ (tA(AGC)F)*, *tDNA$^{tyr}$ (tY(GUA)F1*, and *tDNA$^{gly}$ (tG(GCC)J2*], one telomere site (Tel VI-R), and the ectopic CEN7 site from (B and C). The data for CEN7 are the same as in (C) but shown at a different scale. Blue bar indicates the binding of Rrm3. Red bar indicates the binding of Rrm3-K260A. The orange bars are the values from untagged strains. All data in (B, C, and D) are presented as [ChIP/Input] at the target sites (for historic reasons, binding was not normalized to *YBL028C*); error bars are one SD from the average for three independent experiments. ChIP, chromatin immunoprecipitation; NS, not significant; qPCR, quantitative PCR.

later (75 min; Figure 3D, blue squares). Together, these data are consistent with a model where Rrm3 action at centromeres occurs during the time of centromere replication, while ScPif1 acts after centromere replication. The fact that ScPif1 binding to all three centromeres occurred in a more discrete manner than Rrm3 binding provides additional support for its being a non-S phase event.

### *The cell cycle timing of Rrm3 and ScPif1 binding to centromeres is altered in the absence of the other helicase*

Next, we examined the timing of Rrm3 binding to centromeres in cells lacking ScPif1 and ScPif1 centromere binding in *rrm3*Δ cells. For these experiments, we used the *pif1-m2* allele, even though it is not a complete null for nuclear functions, rather than *pif1*Δ, because the doubling time of *pif1-m2* cells, which are respiratory proficient, is similar to WT while the respiratory-deficient *pif1*Δ cells grow slowly (Schulz and Zakian 1994; Zhou *et al.* 2000) (Figure 4O).

If the two helicases compensate for the absence of the other helicase, we anticipated that Rrm3 binding will occur later and ScPif1 earlier in the cell cycle in the mutant compared to WT cells. Indeed, while Rrm3 still bound CEN3 and CEN12 at early time points (0–30 min), Rrm3 binding to these centromeres was significantly higher ($P < 0.05$) in *pif1-m2* than in WT cells in late S and post-S phase time points (45–75 min; Figure 3, A and E; purple diamonds). At CEN11, Rrm3 binding was still high from 0 to 30 min in *pif1-m2* cells, but was even higher in late S phase [binding at 45, 60, and 75 min was significantly higher ($P < 0.05$) than in WT cells; Figure 3C, purple diamonds].

Likewise, the cell cycle pattern of ScPif1 binding to the three centromeres was altered in the absence of Rrm3. At CEN3 (Figure 3B, green triangles), ScPif1 binding was significantly higher at 30 and 45 min, and significantly lower at 60 and 75 min in *rrm3*Δ compared to WT cells ($P < 0.05$). Similarly, at CEN12, the peak of ScPif1 binding shifted from 60 to 45 min in *rrm3*Δ cells, and was significantly higher at these time points when compared to WT cells (Figure 3F, green triangles, $P < 0.05$). At CEN11, ScPif1 binding was significantly higher at 45 min and significantly lower at 75 min in *rrm3*Δ compared to WT cells (Figure 3D, green triangles, $P < 0.01$).

Taken together, these results suggest the following model. In WT cells, Rrm3 binds centromeres mainly during their time of replication, while ScPif1 binds mainly after centromere replication in late S/G2 phase. However, the shift of binding

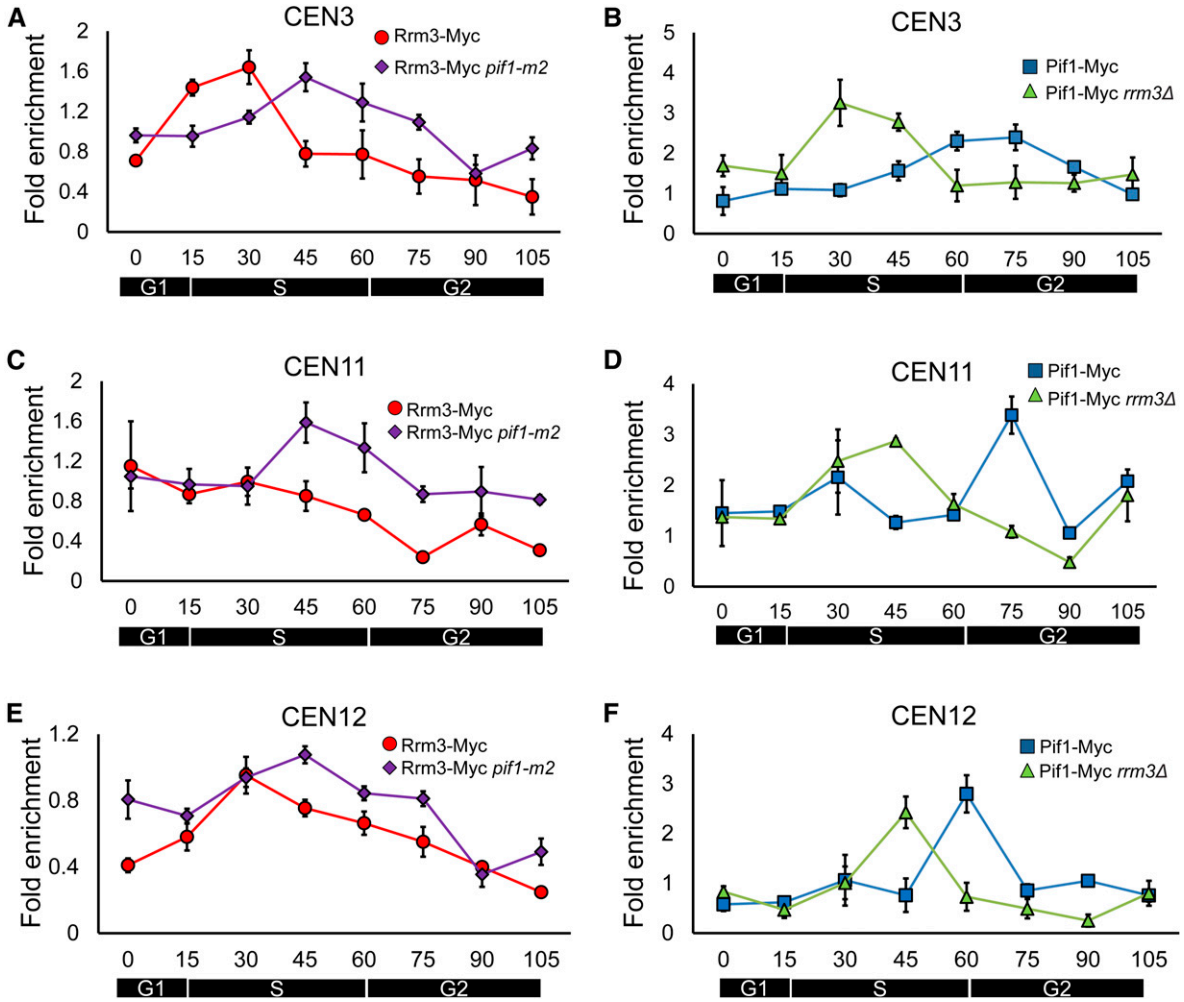


**Figure 3** ScPif1 and Rrm3 binding to centromeres is cell cycle regulated. Cells, which were grown at 24° throughout the experiment, were arrested by incubation in α-factor and then released to proceed through the cell cycle. Samples were collected for ChIP-qPCR and FACS at indicated times ($T$ = 0, 15, 30, 45, 60, 75, 90, and 105 min). Immunoprecipitated DNA was purified and analyzed by qPCR. Data are presented as [(ChIP/Input)$_{\text{Target site}}$/(ChIP/Input)$_{YBL028C}$]. Error bars are 1 SD from the average value of three independent experiments. (A) Rrm3 binding to CEN3 throughout a synchronous cell cycle in WT cells (red circles) or in *pif1-m2* cells (purple diamonds). (B) ScPif1 binding to CEN3 throughout a synchronous cell cycle in WT cells (blue squares) or in *rrm3*Δ cells (green triangles). (C) Same as (A) except Rrm3 binding is to CEN11. (D) Same as in (B) except that ScPif1 binding is to CEN11. (E) Same as (A) except Rrm3 binding is to CEN12. (F) Same as in (B) except that ScPif1 binding is to CEN12. ChIP, chromatin immunoprecipitation; qPCR, quantitative PCR; WT, wild-type.

profiles to later in the cell cycle for Rrm3 in *pif1-m2* cells and earlier in the cell cycle for ScPif1 in *rrm3*Δ cells, suggests that Rrm3 is able to compensate for the post-S phase function of ScPif1 when ScPif1 is absent and vice versa. Alternatively, time of centromere replication might be altered in the absence of Rrm3 or Pif1.

### *ScPif1 promotes replication through centromeres but only in rrm3Δ cells*

Recently ScPif1 was found to promote fork progression at tDNAs, but only in *rrm3*Δ cells (Osmundson *et al.* 2017; Tran *et al.* 2017). To test if ScPif1 promotes replication of centromeres, we examined fork progression at centromeres in mutant and WT cells at CEN6 and CEN11 using 2D gel electrophoresis (2D gel) analysis in asynchronous cells (Figure 4).

The pattern of replication intermediates for CEN6 reflects the fact that two origins contribute to its replication. In some cells, it is replicated by forks moving from *ARS605* and in others from *ARS606* (Figure 4B). When replication occurs from *ARS605*, forks move from left to right through the *Mfe*I fragment examined by 2D gels; when replication occurs from *ARS606*, forks move right to left through the same fragment. As both origins are outside the *Mfe*I fragment (Figure 4B), replication from either origin produces a simple Y-shaped structure of identical size and shape (Figure 4A cartoon). However, two pause sites are visible on the arc of replication intermediates, one for each origin. The stronger pause (marked by solid arrow on the cartoon) arises from forks that begin at *ARS605*, as it is closer than *ARS606* to CEN6. The more minor pause (marked with a dotted arrow) is due to forks that initiate from *ARS606*. Because the

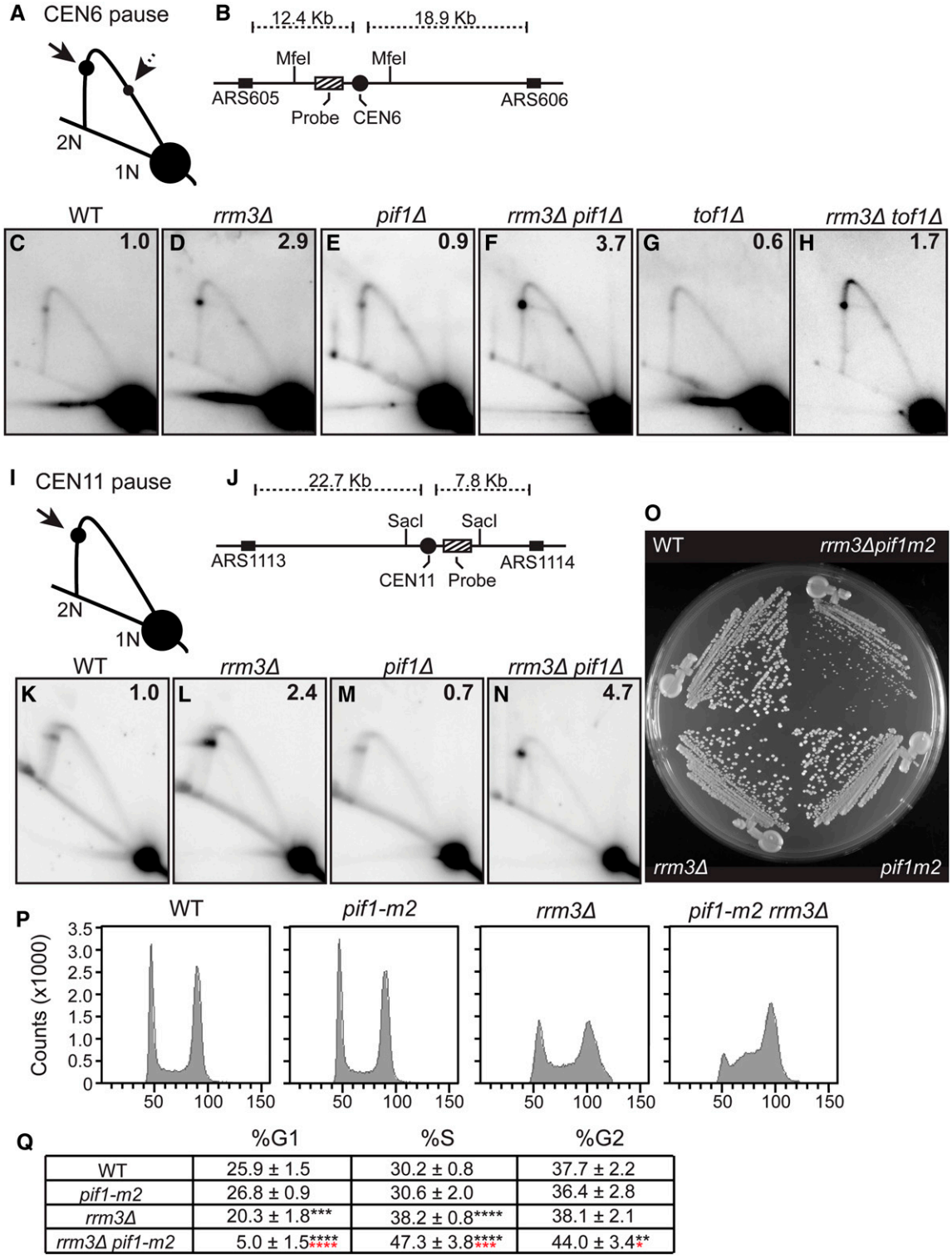


Q

| | %G1 | %S | %G2 |
|---|---|---|---|
| WT | 25.9 ± 1.5 | 30.2 ± 0.8 | 37.7 ± 2.2 |
| *pif1-m2* | 26.8 ± 0.9 | 30.6 ± 2.0 | 36.4 ± 2.8 |
| *rrm3Δ* | 20.3 ± 1.8*** | 38.2 ± 0.8**** | 38.1 ± 2.1 |
| *rrm3Δ pif1-m2* | 5.0 ± 1.5**** | 47.3 ± 3.8*** | 44.0 ± 3.4** |

**Figure 4** ScPif1 promotes replication through centromeres but only in *rrm3*Δ cells. DNA from asynchronous WT and mutant cells was analyzed by 2D gel electrophoresis and Southern blot hybridization. (A) Schematic of 2D gel signal of *Mfe*I-digested DNA using the probe indicated in (B) for the CEN6 fragment. Arrows mark the pauses at CEN6 along the arc of Y-shaped replication intermediates. The solid arrow indicates the pause produced from replication forks originating from *ARS605*. The dashed arrow indicates the pause arising from forks originating from *ARS606*. 1N indicates non-replicating linear *Mfe*I fragments. 2N indicates near fully replicated MfeI fragments. (B) Schematic of the *Mfe*I fragment that contains CEN6 in relation to the flanking replication origins. Cross-hatch box indicates the position of the radiolabeled probe used for Southern blot analysis. (C–H) Southern blot analysis of 2D gels on CEN6 from cells with the following genotypes: (C) WT, (D) *rrm3*Δ, (E) *pif1*Δ, (F) *rrm3*Δ *pif1*Δ, (G) *tof1*Δ, and (H) *rrm3*Δ *tof1*Δ. (I) Same as (A) except that schematic is of CEN11 on a *Sac*I fragment. (J) Same as (B) except that it shows CEN11 in relation to the flanking replication origins. (K–N) Southern blot of 2D gels from the following strains: (K) WT, (L) *rrm3*Δ, (M) *pif1*Δ, and (N) *rrm3*Δ *pif1*Δ. For both CEN6 and CEN11, the

qualitative effects of different mutations were the same at the two pause sites, quantification was done only on the major pause site. For both CEN6 and CEN11, pausing in WT cells was defined as one (see legend for Figure 4). The level of pausing relative to pausing in WT cells is indicated in the upper right corner of each 2D gel panel.

As expected (Greenfeder and Newlon 1992), 2D gel analysis demonstrated modest fork pausing at CEN6 in WT cells (Figure 4C) and a 2.9-fold increase in this pausing in *rrm3*Δ cells (Figure 4D) (Ivessa *et al.* 2003). In *pif1*Δ cells, the extent of replication fork pausing at CEN6 was similar to that seen in WT cells (0.9 times the WT level; Figure 4E). However, pausing at CEN6 in *pif1*Δ *rrm3*Δ cells was 3.7 times higher than in WT cells (Figure 4F). We also tested pausing at CEN6 in *tof1*Δ and *rrm3*Δ *tof1*Δ cells (Figure 4, G and H). Consistent with earlier data (Hodgson *et al.* 2007), forks still paused at CEN6 in *tof1*Δ cells, but the pausing was 0.6 times that seen in WT cells. In addition, pausing at CEN6 was lower in *rrm3*Δ *tof1*Δ cells than in *rrm3*Δ cells, suggesting that Tof1 and Rrm3 act antagonistically at centromeres as they do at the RFB (Mohanty *et al.* 2006; Hodgson *et al.* 2007).

The results were similar at CEN11 (Figure 4, K–N). Pausing was 2.4-fold higher in *rrm3*Δ cells (Figure 4L) compared to WT (Figure 4K), and even higher in *pif1*Δ *rrm3*Δ cells (4.7-fold higher than WT; Figure 4N), while pausing in *pif1*Δ cells was even lower than pausing in WT cells (Figure 4M; 0.7 times WT). We conclude that ScPif1 promotes replication through centromeres but only in the absence of Rrm3. Thus, as at tDNAs (Osmundson *et al.* 2017; Tran *et al.* 2017), ScPif1 partially compensates for the absence of Rrm3 during centromere replication.

### *Cells lacking both ScPif1 and Rrm3 are slow growing with an extended S phase*

Rrm3 and ScPif1 have overlapping roles in replication fork progression at tDNAs (Tran *et al.* 2017), G-quadruplex motifs (Paeschke *et al.* 2013), and, as shown here (Figure 4, A–N), during centromere replication (summarized in Table 1). Unpublished work indicates that the two helicases also have overlapping roles in completing DNA replication at converged forks (K. Labib, personal communication). Yet the growth rates of *pif1-m2* and *rrm3*Δ cells were similar to WT (Figure 4O), even though by FACS analysis *rrm3*Δ cells had significantly more cells in S phase (38.2%) than a WT strain (30.2%) ($P = 3 \times 10^{-7}$, Figure 4, P and Q). The double mutant *pif1-m2 rrm3*Δ cells grew much more slowly than WT or single mutants (Figure 4O), and accumulated even more S phase cells (47.3%, $P < 0.001$) (Figure 4, P and Q), consistent with the overlapping roles of the two helicases in multiple aspects of DNA replication.

### *ScPif1 promotes the segregation function of CEN6 but only in the absence of Rrm3*

Centromeres insure proper segregation of the sister chromatids to the two progeny cells. To determine if ScPif1 or Rrm3 binding to centromeres affects their segregation function, we used a centromere plasmid-loss assay in WT and mutant cells (Gibson *et al.* 1990). As a positive control, we monitored CEN plasmid loss in *cbf1*Δ cells, as Cbf1 is needed for the full segregation function of budding yeast centromeres (Mellor *et al.* 1990). We measured the loss of pRS316, a CEN6 *URA3* plasmid, during growth in nonselective media (Figure 5). Consistent with earlier results, loss of pRS316 in *cbf1*Δ cells was ~3.4-fold higher than in WT cells ($P < 0.0001$). pRS316 loss was also higher in *rrm3*Δ cells (~2.0-fold increase over WT, $P < 0.0001$), although not as high as in *cbf1*Δ cells. In contrast, CEN plasmid loss was indistinguishable ($P > 0.05$) between WT and *pif1*Δ or *pif1*-m2 cells. Thus, in otherwise WT cells, ScPif1 does not affect the segregation rate of a CEN6 plasmid. However, as with fork progression, ScPif1 appears to compensate for Rrm3 during segregation, as CEN plasmid loss was significantly higher in *pif1-m2 rrm3*Δ or *pif1*Δ *rrm3*Δ cells (around threefold, $P < 0.001$) than in *rrm3*Δ cells.

### *The absence of Rrm3 renders cells resistant to microtubule-destabilizing drugs and suppresses the sensitivity of other strains to these drugs*

To test the idea that ScPif1 has a function in sister chromatid separation, we asked if the absence of ScPif1 and/or Rrm3 affected sensitivity to two microtubule inhibitors, benomyl (Figure 6A) and nocodazole (Figure S3). Although the positive control *cbf1*Δ was, as expected, benomyl-sensitive, *pif1-m2* and *pif1*Δ cells grew as well as WT cells on 10 μg/ml benomyl (Figure 6A). However, *rrm3*Δ cells were resistant to benomyl, and deletion of *RRM3* conferred benomyl resistance to both *pif1-m2* and *cbf1*Δ cells (Figure 6A). Cells expressing the helicase-dead *rrm3-K260A* allele were also benomyl-resistant. Thus, Rrm3 ATPase activity is required for sensitivity to microtubule inhibitors. Similar results were obtained for cells grown on 10 μg/ml nocodazole, except that *pif1-m2* cells were modestly resistant to nocodazole and *pif1-m2* did not suppress the nocodazole sensitivity of *cbf1*Δ cells (Figure S3).

signal at the pause was quantified as in Tran *et al.* (2017) and normalized to the pause signal in WT cells to obtain the relative fold change. The average fold difference of mutant over WT from two or more independent biological replicates is shown in the upper right corner of each Southern blot. (O) Freshly dissected WT, *pif1-m2*, *rrm3*Δ, and *pif1-m2 rrm3*Δ spore clones derived from a multiply heterozygous but otherwise isogenic diploid were streaked on YEPD plate at 30° for 2 days. (P) Representative FACS profiles for one of five spore clones from WT, *pif1-m2*, *rrm3*Δ, and *pif1-m2 rrm3*Δ cells. (Q) Quantified FACs data from five independent biological replicates of each strain that were grown asynchronously at 30°. The percent of cells from each strain that are in G1, S, and G2 phase are indicated along with statistical significance relative to WT cells; indicated by black asterisks. Statistical significance of *pif1-m2 rrm3*Δ relative to *rrm3*Δ is indicated by red asterisks. * $P \leq 0.05$, ** $P \leq 0.01$, *** $P \leq 0.001$, **** $P \leq 0.0001$. 2D, two-dimensional; WT, wild-type; YEPD, YEP and dextrose.

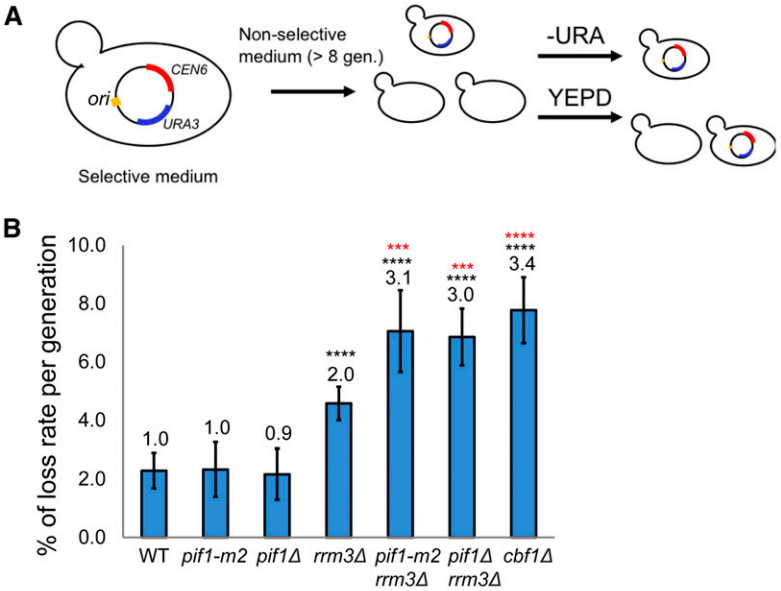


C

| Genotype | % URA cells after 0 generation | % URA cells after N generation | No. of generations | Average plasmid loss rate per cell and generation |
|---|---|---|---|---|
| WT | 96 ± 2 | 74 ± 2 | 11 | $2.3 \times 10^{-2}$ |
| *cbf1Δ* | 67 ± 5 | 33 ± 6 | 8.5 | $7.8 \times 10^{-2}$ |
| *pif1-m2* | 96 ± 2 | 73 ± 3 | 11 | $2.3 \times 10^{-2}$ |
| *pif1Δ* | 97 ± 4 | 78 ± 3 | 10 | $2.2 \times 10^{-2}$ |
| *rrm3Δ* | 86 ± 4 | 54 ± 3 | 10 | $4.6 \times 10^{-2}$ |
| *pif1-m2 rrm3Δ* | 74 ± 5 | 40 ± 4 | 8.5 | $7.1 \times 10^{-2}$ |
| *pif1Δ rrm3Δ* | 76 ± 4 | 41 ± 4 | 8.5 | $6.9 \times 10^{-2}$ |

**Figure 5** ScPif1 family helicases promote the segregation function of CEN6. (A) Schematic of CEN plasmid-loss assay. (B) Loss rate of CEN plasmid per generation in indicated strains. The loss rate in WT cells is defined as one and loss rates in mutant strains were normalized to this value. Means and SD of plasmid loss were obtained from a least three technical replicates of three different isolates per strain; *** $P \leq 0.001$ and **** $P \leq 0.0001$. Black asterisks indicate the significance of the loss rate in mutant *vs.* WT cells. Red asterisks indicate significance between the indicated mutant and *rrm3Δ* cells. (C) The table shows absolute plasmid loss rates in different strains. The average plasmid loss rate (R) is calculated per cell and number of generations. $R = 1 - (F/I)^{1/N}$. I = the percentage of plasmid-containing cells at 0 generation. F = the percentage of plasmid-containing cells after *N* generations. WT, wild-type.

We also tested if Rrm3 or ScPif1 binding to centromeres was affected by benomyl (Figure 6, B–D). While there were several modest differences in binding in these assays, the only dramatic effect was significantly higher ($P < 0.001$) ScPif1 binding to CEN3, 12, and 13 in *rrm3Δ* cells (Figure 6, B–D). ScPif1 binding to two tDNAs was not affected significantly by benomyl even in *rrm3Δ* cells (Figure 6, E and F, $P > 0.05$).

## Discussion

There is growing interest in Pif1 family helicases owing to their multiple and diverse roles in promoting genome integrity (Table 1). This study extends the known functions of ScPif1 by showing that it affects centromere replication and segregation in *rrm3Δ* cells (Figures 4 and 5). Moreover, this study provides another example of ScPif1 and Rrm3 having overlapping functions at hard-to-replicate sites.

A role for ScPif1 at centromeres was first suggested by its robust binding to all 16 yeast centromeres by genome-wide ChIP-seq carried out in asynchronous cells (Figure 1, B and C). ChIP-qPCR confirmed these findings at 6 of the 16 yeast centromeres (Figure 1D and Figure 2B). As Rrm3 moves with the replisome, it binds to all nuclear sequences at their time of replication (Azvolinsky *et al.* 2006). However, in asynchronous cells, its binding to centromeres was 5–10-fold higher than to a control sequence (Figure 1D). Higher Rrm3 binding is also seen at other hard-to-replicate sites, such as tDNAs and telomeres (Azvolinsky *et al.* 2009; Tran *et al.* 2017) (Figure 2D). This higher Rrm3 binding to Rrm3-affected sites is likely due to the pausing of the replisome at these sequences, even in WT cells (Azvolinsky *et al.* 2009). Alternatively, or in addition, more Rrm3 may be recruited to hard-to-replicate sites when the fork stops (rather than pauses) at the site, requiring additional Rrm3 to relieve replication fork arrest. We speculate that the reduced binding of the catalytically dead Rrm3-K260A to multiple Rrm3-affected sites, including centromeres, may reflect a defect of the mutant protein in its recruitment, or the stability of its binding to a stalled or arrested fork (Figure 2, C and D).

Neither Rrm3 nor ScPif1 bound strongly to a mutant CEN7 with a nonfunctional CDEIII element (Figure 2B). For Rrm3, the low binding is expected as a mutant CEN does not impede fork progression (Greenfeder and Newlon 1992). In contrast to Rrm3, ScPif1 was recruited to centromeres after their replication (Figure 3, B, D, and F), a pattern also seen at G4 motifs (Paeschke *et al.* 2011). Reduced ScPif1 binding to nonfunctional centromeres suggests that some aspect of a functional centromere, such as the Cbf3 complex (see *Introduction*), is needed to recruit ScPif1 to the kinetochore. The finding that the centromere binding of Rrm3, but not ScPif1, was significantly higher in *tof1Δ* cells (Figure 1E) suggests that, in WT cells, the two helicases have different centromere functions and that at least one Rrm3 function involves displacement of the multiprotein kinetochore complex during DNA replication.

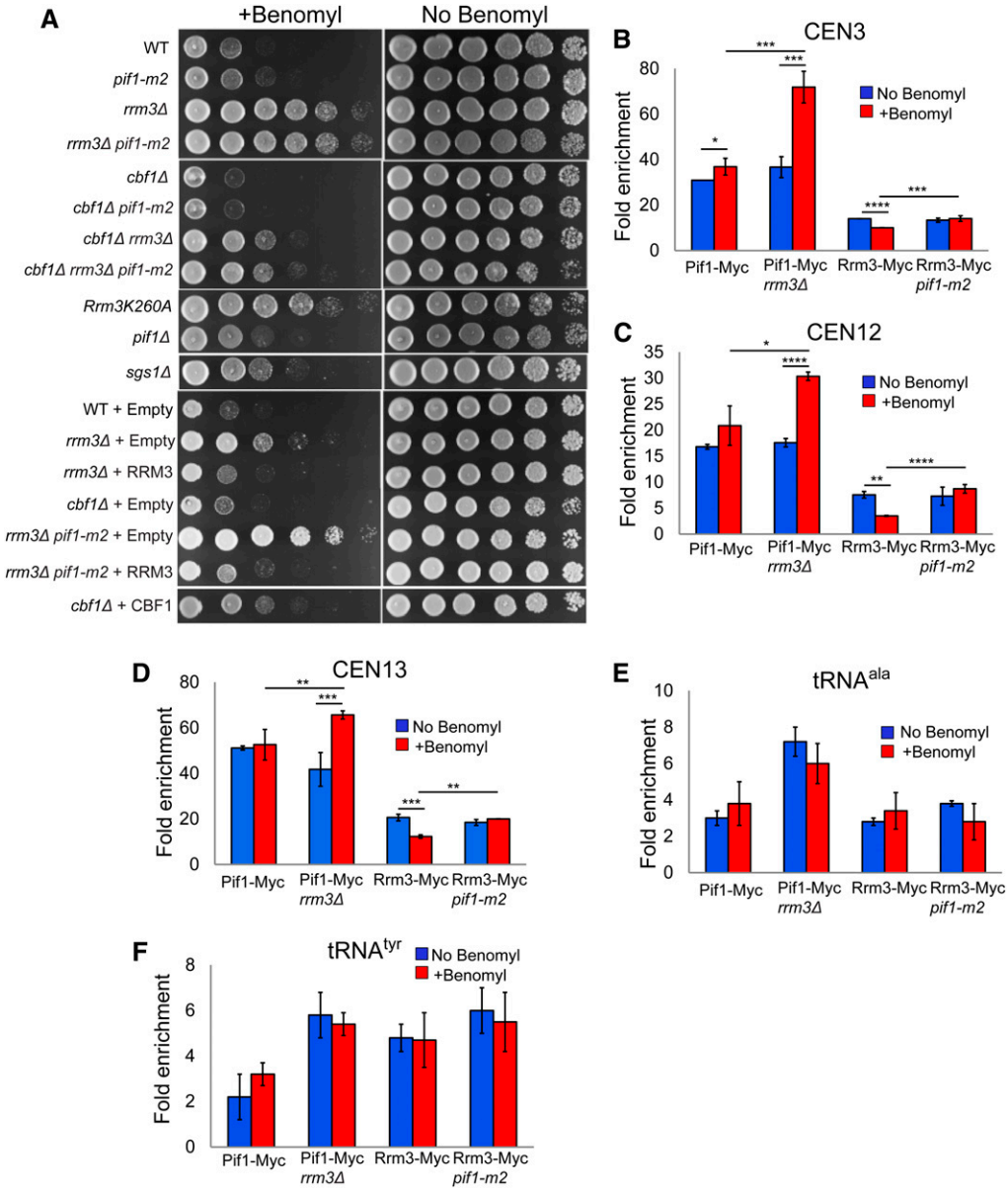


**Figure 6** Effects of benomyl on growth and helicase centromere binding in the presence and absence of Pif1 family helicases. (A) Strains of the indicated genotype were spotted in fivefold serial dilutions on YEPD plates containing no or 10 μg/ml benomyl. (B–F) The indicated strains were treated with or without benomyl, and analyzed by ChIP-qPCR. Each strain was tested in triplicate by ChIP-qPCR using three biological replicates. * $P \leq 0.05$, ** $P \leq 0.01$, *** $P \leq 0.001$, and *** $P \leq 0.0001$. (B) CEN3, (C) CEN12, (D) CEN13, (E) $tRNA^{ala}$, and (F) $tRNA^{tyr}$. ChIP, chromatin immunoprecipitation; qPCR, quantitative PCR; WT, wild-type; YEPD, YEP and dextrose.

The idea that the two helicases do not have the same function at centromeres is also supported by their different temporal patterns of centromere binding (Figure 3). Rrm3 binding occurred mainly in early–mid-S phase, while ScPif1 binding occurred at the end of or even after S phase, when centromere replication is complete. Consistent with these binding patterns, Rrm3 promotes centromere replication (Ivessa *et al.* 2003) while ScPif1 did not in WT cells (Figure 4). The temporal pattern of centromere binding was altered for both helicases when the other helicase was absent, earlier in the cell cycle for ScPif1 in *rrm3*Δ cells and later in the cell cycle for Rrm3 in *pif1-m2* cells (Figure 3). The earlier centromere binding of ScPif1 in *rrm3*Δ cells is consistent with the 2D gel data showing that ScPif1 promoted centromere replication in the absence of Rrm3 (Figure 4).

The effects of mutating the two helicases on the segregation of centromere plasmids was similar to their effects on centromere replication (Figure 5). The loss rate of a centromere plasmid was two-times higher in *rrm3*Δ compared to WT cells, a significant increase. However, loss of centromere plasmids was not affected by the absence of ScPif1, except in cells that also lacked Rrm3. The most parsimonious explanation for the segregation defects in *rrm3*Δ and *rrm3*Δ *pif1-m2* (and *rrm3*Δ *pif1*Δ) cells is that it is a secondary consequence of the impaired centromere replication in these backgrounds (Figure 4). However, we cannot exclude a more direct role for one or both helicases in centromere segregation. Indeed, the temporal pattern of ScPif1 centromere binding in late S/G2 phase suggests that ScPif1 (and perhaps Rrm3 in *pif1-m2* cells) has a non-S phase centromere function (Figure 3). The timing of this binding hints at the possibility that the

**Table 1 Functions of Pif1 family helicases**

| | Pif1 | Rrm3 | Pfh1 |
|---|---|---|---|
| Replication fork progression | | | |
| tDNAs | B (1) | Y (2) | Y (3) |
| G4 motifs | Y (4) | B (5) | Y (6) |
| Centromeres | B (7) | Y (2) | NT |
| Telomeres | (N) | Y (8) | Y (9) |
| RFB | N (10) | Y (10) | Y (3) |
| Support RFB | Y (10) | N (10) | N (3) |
| Separate converged forks | Y (11) | Y (10, 12) | Y (3, 13) |
| Maintain mtDNA | Y (14) | N | Y (15) |
| Inhibit telomerase | Y (16) | N (8) | N (9) |
| Promote BIR | Y (17) | N (17) | NT |
| Process Okazaki fragments | Y (18) | Y (19) | NT |

References used: (1) Tran *et al.* 2017; Osmundsen *et al.* 2017; (2) Ivessa *et al.* 2003; (3) Sabouri *et al.* 2012; (4) Paeschke *et al.* 2011; Lopes *et al.* 2011; (5) Paeschke *et al.* 2013; (6) Sabouri *et al.* 2014; (7) This paper; (8) Ivessa *et al.* 2002; (9) McDonald *et al.* 2014; (10) Ivessa *et al.* 2000; (11) K. Labib, personal communication; (12) Fachinette *et al.* 2010; (13) Steinacher *et al.* 2012; (14) Foury and Kolodynski 1983; (15) Pinter *et al.* 2008; (16) Zhou *et al.* 2000; (17) Saini *et al.* 2003; Wilson *et al.* 2013; (18) Budd *et al.* 2006; and (19) Osmundsen *et al.* 2017. B, Backup role; Y, Yes; NT, not tested; (N), probably no; RFB, replication fork barrier; N, NO; BIR, break-induced replication.

additional function could be promoting sister chromatid separation. We tested this idea by asking if a lack of ScPif1 affected benomyl or nocodazole sensitivity (Figure 6 and Figure S3). Contrary to our model, *pif1-m2* and *pif1*Δ cells had WT sensitivity to benomyl and were modestly nocodazole-resistant, while *rrm3*Δ cells were benomyl- and nocodazole-resistant, as were *rrm3*Δ *pif1-m2* cells. We do not know why these strains were resistant to microtubule inhibitors but speculate that in *rrm3*Δ and *rrm3*Δ *pif1-m2* cells, it is linked to their longer S phase (Figure 4, P and Q).

Despite Pif1-deficient cells having WT benomyl sensitivity, we still favor the idea that ScPif1 affects centromere segregation. However, if ScPif1 were the major player in promoting a key step in sister chromatid separation, the absence of ScPif1 alone should negatively impact the segregation of centromere plasmids, yet the rate of centromere plasmid loss in *pif1*Δ cells was the same as in WT cells (Figure 5). Therefore, if ScPif1 contributes to a function that is important for the segregation of centromeres, it must share this function with another protein, perhaps a helicase, other than Rrm3. However, a synthetic screen to identify nonessential genes that are synthetically lethal or sick in a *pif1-m2* background did not identify any of the over 100 nonessential genes that have helicase motifs (Stundon and Zakian 2015). We suggest from the cell cycle pattern of Rrm3 binding in *pif1-m2* cells (Figure 3, A, C, and E) that Rrm3 might carry out the late cell cycle activity of ScPif1 in *pif1-m2* cells. However, *rrm3*Δ *pif1-m2* cells are benomyl- and nocodazole-resistant (Figure 6A and Figure S3), which is not expected if the two helicases cooperate to promote sister chromatid separation. One interaction that came out of the *pif1-m2* synthetic screen (Stundon and Zakian 2015) that might be relevant to a post-S phase function for ScPif1 at centromeres was the lethality of *pif1-m2 cdh1*Δ cells. Cdh1 is an activator of the APC (anaphase-promoting complex) that drives cells into anaphase, in part by leading to the release of cohesin from the centromeres of sister chromatids (Biggins 2013). Perhaps, ScPif1 and Cdh1 both contribute to cohesion removal, with ScPif1 providing a "push" that enhances the actions of Cdh1. The synthetic lethality of the double mutant may also be related to higher levels of ScPif1 in cells lacking APC function (Vega *et al.* 2007).

In summary, Rrm3 and ScPif1 bound centromeres at different times in the cell cycle, and this timing was influenced by the other helicase in a manner that would allow either helicase to compensate at least in part for the loss of the other. Rrm3 had the major role in replication through the multiprotein kinetochore complex. ScPif1 also promoted centromere replication, but its replication function was detected only in *rrm3*Δ cells. These roles in replication provide a plausible explanation for the positive effects of these helicases on the segregation fidelity of centromere plasmids.

Unlike *S. cerevisiae*, most eukaryotes encode only one Pif1 family helicase. The single *S. pombe* Pif1 family helicase, Pfh1, has an as yet unidentified essential nuclear function (Pinter *et al.* 2008). With the exception of telomerase inhibition (McDonald *et al.* 2014), Pfh1 carries out all of the tested functions of ScPif1 and Rrm3 (Table 1) (Foury and Kolodynski 1983; Tanaka *et al.* 2002; Zhou *et al.* 2002; Ryu *et al.* 2004; Budd *et al.* 2006; Fachinetti *et al.* 2010; Lopes *et al.* 2011; Sabouri *et al.* 2012, 2014; Steinacher *et al.* 2012; Saini *et al.* 2013; McDonald *et al.* 2014, 2016; Wallgren *et al.* 2016; Mohammad *et al.* 2018). However, a possible role for Pfh1 in centromere replication has not, to our knowledge, been examined. *S. pombe* centromeres are much larger and more complex than the budding yeast point centromere (Yamagishi *et al.* 2014). Thus, it is possible that a role for Pfh1 in centromere replication could explain why Pfh1 is essential for the integrity of nuclear DNA (Pinter *et al.* 2008), while *pif1*Δ *rrm3*Δ are slow growing but viable (Figure 4O). The conservation of multiple functions that affect genome integrity among the Pif1 family helicases in *S. cerevisiae* and *S. pombe*, two evolutionarily distant yeast species, raises the possibility that these helicases might have similar functions in multicellular eukaryotes.

## Acknowledgments

We thank Sue Biggins and Kerry Bloom for useful discussions; Carly L. Geronimo and Angela Chan for their careful reading of the manuscript; C. J. Decoste and the Princeton Molecular Biology FACS facility for technical help. This work was funded by grant 1R35 GM-118279 to V.A.Z. from the National Institutes of Health. C.-F.C. was funded in part by a grant from the New Jersey Commission on Cancer Research (NJCCR). T.J.P. was funded in part by grants from the Ford Foundation, the Burroughs Wellcome Fund Postdoctoral Enrichment Program, and the NJCCR. The authors declare no conflict of interest.

Author contributions: All authors contributed to the design and interpretation of experiments. C.-F.C. carried out all of the ChIP, plasmid segregation, and microtubule inhibitor experiments. T.J.P. carried out the 2D gels and cell cycle data in Figure 4. S.P. analyzed the ChIP-seq experiments and prepared Figure 1, B and C. C.-F.C., T.J.P., and V.A.Z. wrote the manuscript. All authors contributed to scientific discussion and critical revisions of the manuscript.

## Literature Cited


Akalin, A., V. Franke, K. Vlahovicek, C. E. Mason, and D. Schubeler, 2015 Genomation: a toolkit to summarize, annotate and visualize genomic intervals. Bioinformatics 31: 1127–1129. https://doi.org/10.1093/bioinformatics/btu775

Azvolinsky, A., S. Dunaway, J. Z. Torres, J. B. Bessler, and V. A. Zakian, 2006 The S. cerevisiae Rrm3p DNA helicase moves with the replication fork and affects replication of all yeast chromosomes. Genes Dev. 20: 3104–3116. https://doi.org/10.1101/gad.1478906

Azvolinsky, A., P. G. Giresi, J. D. Lieb, and V. A. Zakian, 2009 Highly transcribed RNA polymerase II genes are impediments to replication fork progression in Saccharomyces cerevisiae. Mol. Cell 34: 722–734. https://doi.org/10.1016/j.molcel.2009.05.022

Bessler, J. B., J. Z. Torres, and V. A. Zakian, 2001 The Pif1p subfamily of helicases: region-specific DNA helicases? Trends Cell Biol. 11: 60–65. https://doi.org/10.1016/S0962-8924(00)01877-8

Biggins, S., 2013 The composition, functions, and regulation of the budding yeast kinetochore. Genetics 194: 817–846. https://doi.org/10.1534/genetics.112.145276

Bochman, M. L., C. P. Judge, and V. A. Zakian, 2011 The Pif1 family in prokaryotes: what are our helicases doing in your bacteria? Mol. Biol. Cell 22: 1955–1959. https://doi.org/10.1091/mbc.e11-01-0045

Boulé, J. B., and V. A. Zakian, 2007 The yeast Pif1p DNA helicase preferentially unwinds RNA DNA substrates. Nucleic Acids Res. 35: 5809–5818. https://doi.org/10.1093/nar/gkm613

Boulé, J. B., L. R. Vega, and V. A. Zakian, 2005 The yeast Pif1p helicase removes telomerase from telomeric DNA. Nature 438: 57–61. https://doi.org/10.1038/nature04091

Brewer, B. J., and W. L. Fangman, 1987 The localization of replication origins on ARS plasmids in S. cerevisiae. Cell 51: 463–471. https://doi.org/10.1016/0092-8674(87)90642-8

Brewer, B. J., and W. L. Fangman, 1991 Mapping replication origins in yeast chromosomes. BioEssays 13: 317–322. https://doi.org/10.1002/bies.950130702

Budd, M. E., C. C. Reis, S. Smith, K. Myung, and J. L. Campbell, 2006 Evidence suggesting that Pif1 helicase functions in DNA replication with the Dna2 helicase/nuclease and DNA polymerase delta. Mol. Cell. Biol. 26: 2490–2500. https://doi.org/10.1128/MCB.26.7.2490-2500.2006

Buzovetsky, O., Y. Kwon, N. T. Pham, C. Kim, G. Ira *et al.*, 2017 Role of the Pif1-PCNA complex in Pol delta-dependent strand displacement DNA synthesis and break-induced replication. Cell Reports 21: 1707–1714. https://doi.org/10.1016/j.celrep.2017.10.079

Chung, W. H., 2014 To peep into Pif1 helicase: multifaceted all the way from genome stability to repair-associated DNA synthesis. J. Microbiol. 52: 89–98. https://doi.org/10.1007/s12275-014-3524-3

Fachinetti, D., R. Bermejo, A. Cocito, S. Minardi, Y. Katou *et al.*, 2010 Replication termination at eukaryotic chromosomes is mediated by Top2 and occurs at genomic loci containing pausing elements. Mol. Cell 39: 595–605. https://doi.org/10.1016/j.molcel.2010.07.024

Foury, F., and J. Kolodynski, 1983 pif mutation blocks recombination between mitochondrial rho+ and rho- genomes having tandemly arrayed repeat units in Saccharomyces cerevisiae. Proc. Natl. Acad. Sci. USA 80: 5345–5349. https://doi.org/10.1073/pnas.80.17.5345

Geronimo, C. L., and V. A. Zakian, 2016 Getting it done at the ends: Pif1 family DNA helicases and telomeres. DNA Repair (Amst.) 44: 151–158. https://doi.org/10.1016/j.dnarep.2016.05.021

Geronimo, C. L., S. P. Singh, R. Galletto, and V. A. Zakian, 2018 The signature motif of the Saccharomyces cerevisiae Pif1 DNA helicase is essential in vivo for mitochondrial and nuclear functions and in vitro for ATPase activity. Nucleic Acids Res. 46: 8357–8370. https://doi.org/10.1093/nar/gky655

Gibson, S. I., R. T. Surosky, and B. K. Tye, 1990 The phenotype of the minichromosome maintenance mutant mcm3 is characteristic of mutants defective in DNA replication. Mol. Cell. Biol. 10: 5707–5720. https://doi.org/10.1128/MCB.10.11.5707

Greenfeder, S. A., and C. S. Newlon, 1992 Replication forks pause at yeast centromeres. Mol. Cell. Biol. 12: 4056–4066. https://doi.org/10.1128/MCB.12.9.4056

Hodgson, B., A. Calzada, and K. Labib, 2007 Mrc1 and Tof1 regulate DNA replication forks in different ways during normal S phase. Mol. Biol. Cell 18: 3894–3902. https://doi.org/10.1091/mbc.e07-05-0500

Huberman, J. A., L. D. Spotila, K. A. Nawotka, S. M. el-Assouli, and L. R. Davis, 1987 The in vivo replication origin of the yeast 2 microns plasmid. Cell 51: 473–481. https://doi.org/10.1016/0092-8674(87)90643-X

Ivessa, A. S., J. Q. Zhou, and V. A. Zakian, 2000 The Saccharomyces Pif1p DNA helicase and the highly related Rrm3p have opposite effects on replication fork progression in ribosomal DNA. Cell 100: 479–489. https://doi.org/10.1016/S0092-8674(00)80683-2

Ivessa, A. S., J. Q. Zhou, V. P. Schulz, E. K. Monson, and V. A. Zakian, 2002 Saccharomyces Rrm3p, a 5′ to 3′ DNA helicase that promotes replication fork progression through telomeric and subtelomeric DNA. Genes Dev. 16: 1383–1396. https://doi.org/10.1101/gad.982902

Ivessa, A. S., B. A. Lenzmeier, J. B. Bessler, L. K. Goudsouzian, S. L. Schnakenberg *et al.*, 2003 The Saccharomyces cerevisiae helicase Rrm3p facilitates replication past nonhistone protein-DNA complexes. Mol. Cell 12: 1525–1536. https://doi.org/10.1016/S1097-2765(03)00456-8

Kent, W. J., C. W. Sugnet, T. S. Furey, K. M. Roskin, T. H. Pringle *et al.*, 2002 The human genome browser at UCSC. Genome Res. 12: 996–1006. https://doi.org/10.1101/gr.229102

Koc, K. N., S. P. Singh, J. L. Stodola, P. M. Burgers, and R. Galletto, 2016 Pif1 removes a Rap1-dependent barrier to the strand displacement activity of DNA polymerase delta. Nucleic Acids Res. 44: 3811–3819. https://doi.org/10.1093/nar/gkw181

Langmead, B., and S. L. Salzberg, 2012 Fast gapped-read alignment with Bowtie 2. Nat. Methods 9: 357–359. https://doi.org/10.1038/nmeth.1923

Lopes, J., A. Piazza, R. Bermejo, B. Kriegsman, A. Colosio *et al.*, 2011 G-quadruplex-induced instability during leading-strand replication. EMBO J. 30: 4033–4046. https://doi.org/10.1038/emboj.2011.316

McCarroll, R. M., and W. L. Fangman, 1988 Time of replication of yeast centromeres and telomeres. Cell 54: 505–513. https://doi.org/10.1016/0092-8674(88)90072-4

McDonald, K. R., N. Sabouri, C. J. Webb, and V. A. Zakian, 2014 The Pif1 family helicase Pfh1 facilitates telomere replication and has an RPA-dependent role during telomere lengthening. DNA Repair (Amst.) 24: 80–86. https://doi.org/10.1016/j.dnarep.2014.09.008

McDonald, K. R., A. J. Guise, P. Pourbozorgi-Langroudi, I. M. Cristea, V. A. Zakian *et al.*, 2016 Pfh1 is an accessory replicative helicase that interacts with the replisome to facilitate fork progression and preserve genome integrity. PLoS Genet. 12: e1006238. https://doi.org/10.1371/journal.pgen.1006238

Mellor, J., W. Jiang, M. Funk, J. Rathjen, C. A. Barnes *et al.*, 1990 CPF1, a yeast protein which functions in centromeres and promoters. EMBO J. 9: 4017–4026. https://doi.org/10.1002/j.1460-2075.1990.tb07623.x

Mohammad, J. B., M. Wallgren, and N. Sabouri, 2018 The Pif1 signature motif of Pfh1 is necessary for both protein displacement and helicase unwinding activities, but is dispensable for strand-annealing activity. Nucleic Acids Res. 46: 8516–8531. https://doi.org/10.1093/nar/gky654

Mohanty, B. K., N. K. Bairwa, and D. Bastia, 2006 The Tof1p-Csm3p protein complex counteracts the Rrm3p helicase to control replication termination of Saccharomyces cerevisiae. Proc. Natl. Acad. Sci. USA 103: 897–902. https://doi.org/10.1073/pnas.0506540103

Muñoz-Galván, S., M. Garcia-Rubio, P. Ortega, J. F. Ruiz, S. Jimeno *et al.*, 2017 A new role for Rrm3 in repair of replication-born DNA breakage by sister chromatid recombination. PLoS Genet. 13: e1006781. https://doi.org/10.1371/journal.pgen.1006781

Natsume, T., C. A. Muller, Y. Katou, R. Retkute, M. Gierlinski *et al.*, 2013 Kinetochores coordinate pericentromeric cohesion and early DNA replication by Cdc7-Dbf4 kinase recruitment. Mol. Cell 50: 661–674. https://doi.org/10.1016/j.molcel.2013.05.011

Osmundson, J. S., J. Kumar, R. Yeung, and D. J. Smith, 2017 Pif1-family helicases cooperatively suppress widespread replication-fork arrest at tRNA genes. Nat. Struct. Mol. Biol. 24: 162–170. https://doi.org/10.1038/nsmb.3342

Paeschke, K., J. A. Capra, and V. A. Zakian, 2011 DNA replication through G-quadruplex motifs is promoted by the Saccharomyces cerevisiae Pif1 DNA helicase. Cell 145: 678–691. https://doi.org/10.1016/j.cell.2011.04.015

Paeschke, K., M. L. Bochman, P. D. Garcia, P. Cejka, K. L. Friedman *et al.*, 2013 Pif1 family helicases suppress genome instability at G-quadruplex motifs. Nature 497: 458–462. https://doi.org/10.1038/nature12149

Pinter, S. F., S. D. Aubert, and V. A. Zakian, 2008 The Schizosaccharomyces pombe Pfh1p DNA helicase is essential for the maintenance of nuclear and mitochondrial DNA. Mol. Cell. Biol. 28: 6594–6608. https://doi.org/10.1128/MCB.00191-08

Pohl, T. J., B. J. Brewer, and M. K. Raghuraman, 2012 Functional centromeres determine the activation time of pericentric origins of DNA replication in Saccharomyces cerevisiae. PLoS Genet. 8: e1002677. https://doi.org/10.1371/journal.pgen.1002677

Quinlan, A. R., and I. M. Hall, 2010 BEDTools: a flexible suite of utilities for comparing genomic features. Bioinformatics 26: 841–842. https://doi.org/10.1093/bioinformatics/btq033

Ribeyre, C., J. Lopes, J. B. Boulé, A. Piazza, A. Guedin *et al.*, 2009 The yeast Pif1 helicase prevents genomic instability caused by G-quadruplex-forming CEB1 sequences in vivo. PLoS Genet. 5: e1000475. https://doi.org/10.1371/journal.pgen.1000475

Ryu, G. H., H. Tanaka, D. H. Kim, J. H. Kim, S. H. Bae *et al.*, 2004 Genetic and biochemical analyses of Pfh1 DNA helicase function in fission yeast. Nucleic Acids Res. 32: 4205–4216. https://doi.org/10.1093/nar/gkh720

Sabouri, N., K. R. McDonald, C. J. Webb, I. M. Cristea, and V. A. Zakian, 2012 DNA replication through hard-to-replicate sites, including both highly transcribed RNA Pol II and Pol III genes, requires the S. pombe Pfh1 helicase. Genes Dev. 26: 581–593. https://doi.org/10.1101/gad.184697.111

Sabouri, N., J. A. Capra, and V. A. Zakian, 2014 The essential Schizosaccharomyces pombe Pfh1 DNA helicase promotes fork movement past G-quadruplex motifs to prevent DNA damage. BMC Biol. 12: 101. https://doi.org/10.1186/s12915-014-0101-5

Saini, N., S. Ramakrishnan, R. Elango, S. Ayyar, Y. Zhang *et al.*, 2013 Migrating bubble during break-induced replication drives conservative DNA synthesis. Nature 502: 389–392. https://doi.org/10.1038/nature12584

Schulz, V. P., and V. A. Zakian, 1994 The saccharomyces PIF1 DNA helicase inhibits telomere elongation and de novo telomere formation. Cell 76: 145–155. https://doi.org/10.1016/0092-8674(94)90179-1

Steinacher, R., F. Osman, J. Z. Dalgaard, A. Lorenz, and M. C. Whitby, 2012 The DNA helicase Pfh1 promotes fork merging at replication termination sites to ensure genome stability. Genes Dev. 26: 594–602. https://doi.org/10.1101/gad.184663.111

Stundon, J. L., and V. A. Zakian, 2015 Identification of Saccharomyces cerevisiae genes whose deletion causes synthetic effects in cells with reduced levels of the nuclear Pif1 DNA helicase. G3 (Bethesda) 5: 2913–2918. https://doi.org/10.1534/g3.115.021139

Syed, S., C. Desler, L. J. Rasmussen, and K. H. Schmidt, 2016 A novel Rrm3 function in restricting DNA replication via an Orc5-binding domain is genetically separable from Rrm3 function as an ATPase/helicase in facilitating fork progression. PLoS Genet. 12: e1006451. https://doi.org/10.1371/journal.pgen.1006451

Tanaka, H., G. H. Ryu, Y. S. Seo, K. Tanaka, H. Okayama *et al.*, 2002 The fission yeast pfh1(+) gene encodes an essential 5′ to 3′ DNA helicase required for the completion of S-phase. Nucleic Acids Res. 30: 4728–4739. https://doi.org/10.1093/nar/gkf590

Torres, J. Z., J. B. Bessler, and V. A. Zakian, 2004 Local chromatin structure at the ribosomal DNA causes replication fork pausing and genome instability in the absence of the S. cerevisiae DNA helicase Rrm3p. Genes Dev. 18: 498–503. https://doi.org/10.1101/gad.1154704

Tran, P. L. T., T. J. Pohl, C. F. Chen, A. Chan, S. Pott *et al.*, 2017 PIF1 family DNA helicases suppress R-loop mediated genome instability at tRNA genes. Nat. Commun. 8: 15025. https://doi.org/10.1038/ncomms15025

Vega, L. R., J. A. Phillips, B. R. Thornton, J. A. Benanti, M. T. Onigbanjo *et al.*, 2007 Sensitivity of yeast strains with long G-tails to levels of telomere-bound telomerase. PLoS Genet. 3: e105. https://doi.org/10.1371/journal.pgen.0030105

Wallgren, M., J. B. Mohammad, K. P. Yan, P. Pourbozorgi-Langroudi, M. Ebrahimi *et al.*, 2016 G-rich telomeric and ribosomal DNA sequences from the fission yeast genome form stable G-quadruplex DNA structures in vitro and are unwound by the Pfh1 DNA helicase. Nucleic Acids Res. 44: 6213–6231. https://doi.org/10.1093/nar/gkw349

Wilson, M. A., Y. Kwon, Y. Xu, W. H. Chung, P. Chi *et al.*, 2013 Pif1 helicase and Polδ promote recombination-coupled DNA synthesis via bubble migration. Nature 502: 393–396. https://doi.org/10.1038/nature12585

Yamagishi, Y., T. Sakuno, Y. Goto, and Y. Watanabe, 2014 Kinetochore composition and its function: lessons from yeasts. FEMS Microbiol. Rev. 38: 185–200. https://doi.org/10.1111/1574-6976.12049

Zhou, J., E. K. Monson, S. C. Teng, V. P. Schulz, and V. A. Zakian, 2000 Pif1p helicase, a catalytic inhibitor of telomerase in yeast. Science 289: 771–774. https://doi.org/10.1126/science.289.5480.771

Zhou, J. Q., H. Qi, V. P. Schulz, M. K. Mateyak, E. K. Monson *et al.*, 2002 Schizosaccharomyces pombe pfh1+ encodes an essential 5′ to 3′ DNA helicase that is a member of the PIF1 subfamily of DNA helicases. Mol. Biol. Cell 13: 2180–2191. https://doi.org/10.1091/mbc.02-02-0021

Zhou, R., J. Zhang, M. L. Bochman, V. A. Zakian, and T. Ha, 2014 Periodic DNA patrolling underlies diverse functions of Pif1 on R-loops and G-rich DNA. Elife 3: e02190. https://doi.org/10.7554/eLife.02190

*Communicating editor: B. Calvi*